

Supporting Information

Halogen Bonds in 2D Supramolecular Self-Assembly of Organic Semiconductors

Rico Gutzler,^{*a,b} Chaoying Fu,^{b,a} Afshin Dadvand,^{b,a} Yun Hua,^{a,b} Jennifer M. MacLeod,^a Federico Rosei^{*a} and Dmitrii F. Perepichka^{*b}

^a Institut National de la Recherche Scientifique and Centre for Self-Assembled Chemical Structures, Université du Québec, 1650 boulevard Lionel-Boulet, Varennes, QC J3X 1S2, Canada; E-mail: gutzler@emt.inrs.ca, rosei@emt.inrs.ca

^b Department of Chemistry and Centre for Self-Assembled Chemical Structures, McGill University, 801 Sherbrooke Str. West, Montreal, QC H3A 2K6, Canada; E-mail: dmitrii.perepichka@mcgill.ca

Contents

Synthesis of Compound **2**

¹H NMR Spectrum of Compound **1** and MS-APCI of Compound **2**

Natural Bond Orbital Analysis

Additional STM Images

Synthesis of Compound 2

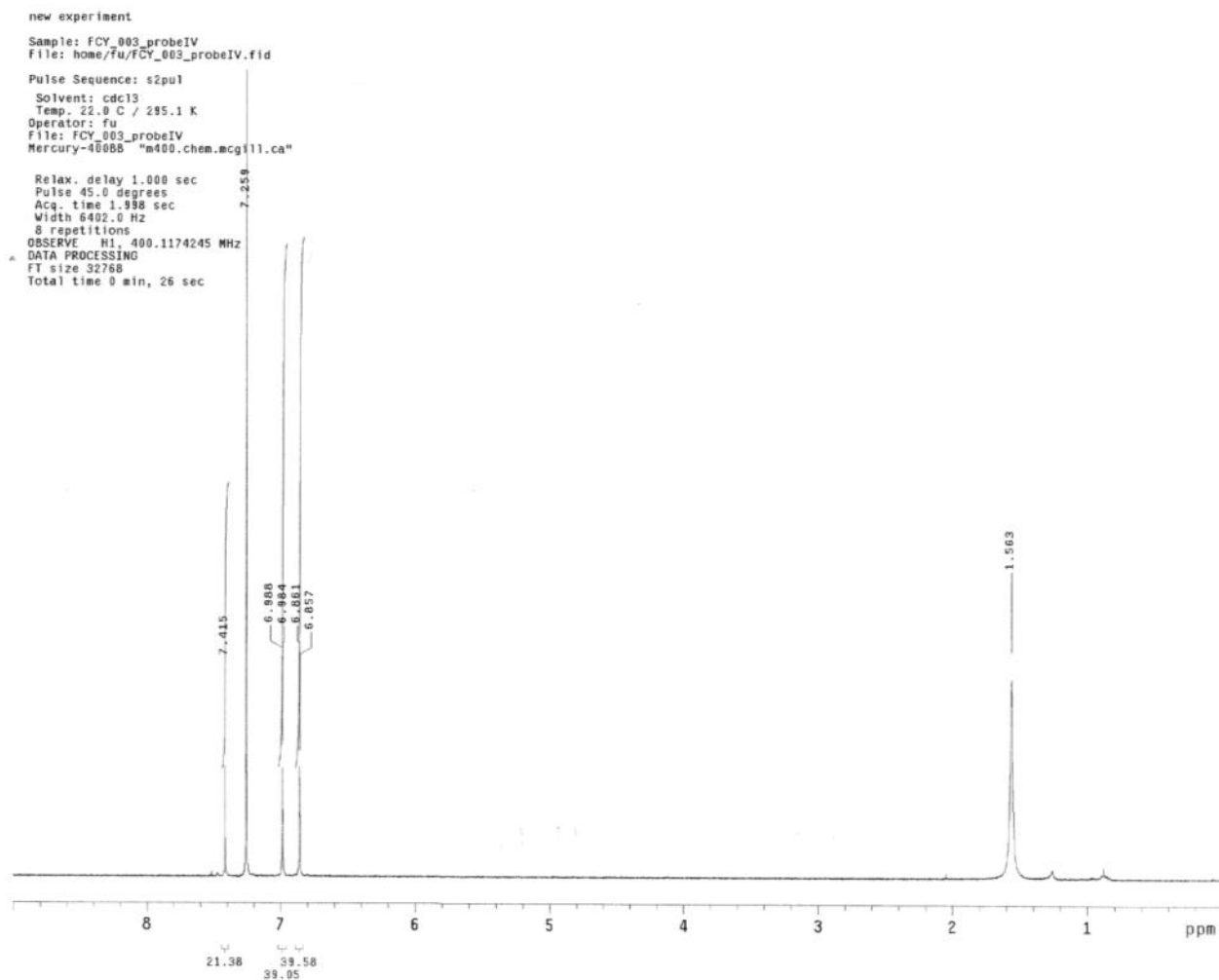
1,2,4,5-tetrakis(5-bromothiophen-3-yl)benzene (I)

A solution of 1,2,4,5-tetra(thiophen-3-yl)benzene⁴⁶ (0.061 g, 0.15 mmol) in dry THF (10.5 mL) was stirred at $-78\text{ }^{\circ}\text{C}$ in N_2 atmosphere while *tert*-butyllithium (0.60 mL, 1.7 M in hexane, 1.0 mmol) was added dropwise. After the reaction mixture was stirred at $-78\text{ }^{\circ}\text{C}$ for 1h, a solution of carbon tetrabromide (0.338 g, 1.02 mmol) in dry THF (2 mL) was added dropwise. The clear dark red solution was stirred and warmed up to room temperature gradually overnight. The reaction mixture was extracted with chloroform (30 mL) and washed with water (50 mL). The organic phase was separated and dried over magnesium sulfate, and the solvent was evaporated, affording **I** as a brown solid (0.052 g, 48%). $^1\text{H NMR}$ (δ , CDCl_3): 7.42 (2H, s), 6.99 (4H, d, $J = 1.6\text{ Hz}$), 6.86 (4H, d, $J = 1.6\text{ Hz}$).

2,5,9,12-tetrabromoanthra[2,1-b:3,4-b':6,5-b'':7,8-b''']tetrathiophene (2)

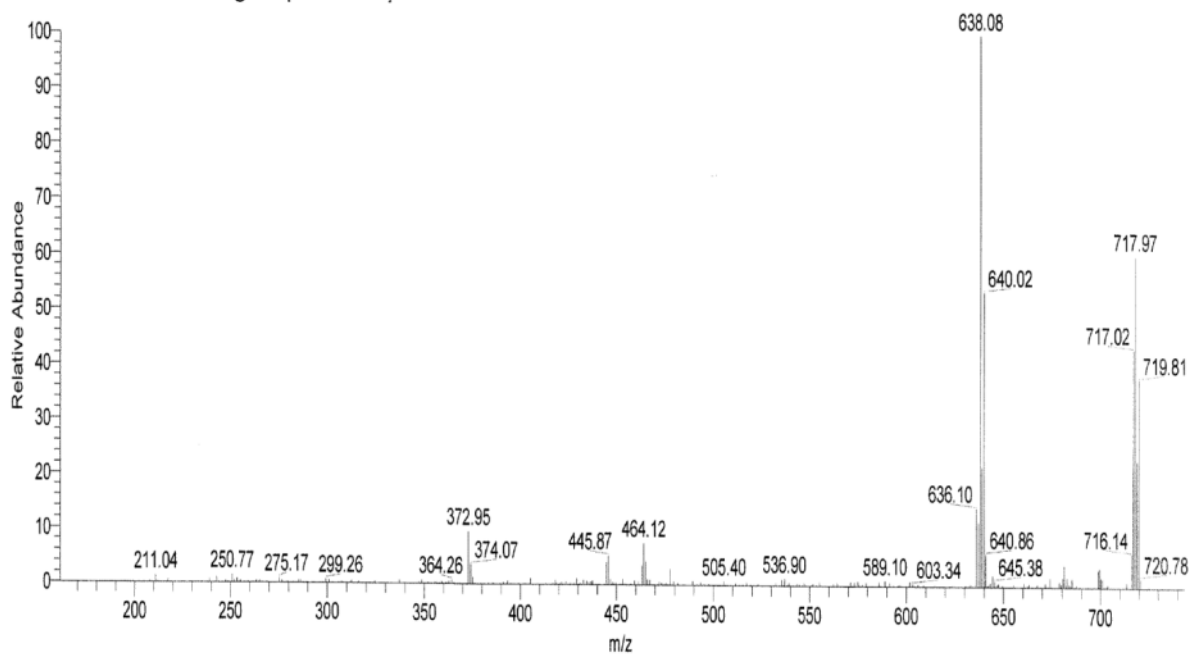
A solution of **I** (0.052 g, 0.072 mmol) in chlorobenzene (10 mL) was stirred while a solution of dry iron(III) chloride (0.070 g, 0.43 mmol) in nitromethane (2 mL) was added. Methanol (60 mL) was added after the reaction mixture was kept stirring for 30 min, and the greenish brown reaction mixture precipitated after 1h. The precipitate was filtered and rinsed with water (0.0354 g, 68.7%), producing crude product **2** as a greenish brown solid. Purification by vacuum sublimation (0.3 mbar, $310\text{ }^{\circ}\text{C}$) afforded the title compound **2** as a yellow crystalline solid (11 mg, 31%). No signal could be detected in solution NMR of **2** due to its extremely low solubility. MS (APCI): m/z : calculated for $[\text{C}_{22}\text{H}_6\text{Br}_4\text{S}_4]$: 717.6032, found: 717.6039.

^1H NMR spectrum of 1,2,4,5-tetrakis(5-bromothiophen-3-yl)benzene (I)



MS-APCI 2,5,9,12-tetrabromoanthra[2,1-b:3,4-b':6,5-b'':7,8-b''']tetrathiophene (2)

091103-01ESIFu-JB3TBrTTA_091103174036 #38-39 RT: 1.01-1.03 AV: 2 NL: 1.29E5
T: + c APCI corona Full ms2 718.00@30.00 [195.00-728.00]



Natural Bond Orbital Analysis

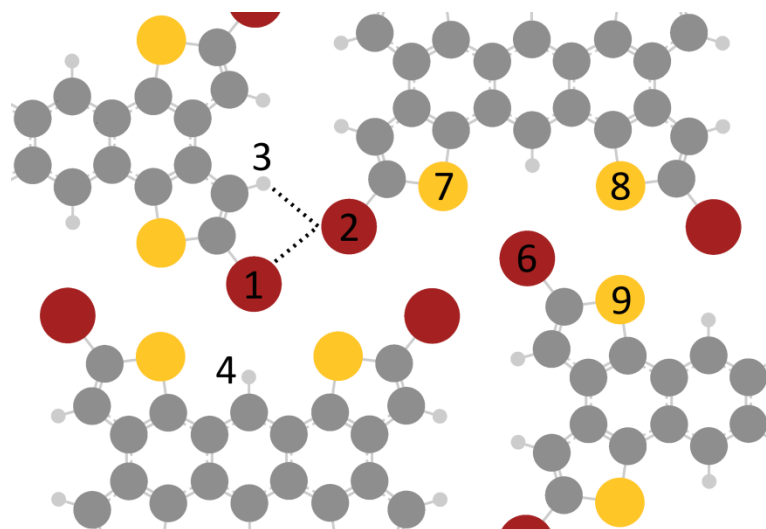
NBO analysis of the three different structures yields several attractive contributions by weak donor–acceptor interactions. The optimized geometries from calculations with the M06-2X functional were used as starting point for NBO analysis (Gaussian NBO Version 3.1¹ implemented in Gaussian 09). Second-order energy lowering $\Delta E^{(2)}$ is given for these interactions along with the interacting orbitals for several close contacts. All of them are interactions between lone pair orbital (n) and antibonding orbitals (σ^*) of adjacent atoms.

The combined halogen⋯halogen and halogen⋯hydrogen bonds (dashed black lines in the following images) yield stabilizing contributions for the three structures. Chalcogen S⋯S contacts contribute less to stabilizing the monolayer, as do Br⋯S contacts. The X₂H synthon dominates intermolecular binding. Labels Dx are given according to the main text.

1 E. D. Glendening, A. E. Reed, J. E. Carpenter, and F. Weinhold, *NBO Version 3.1*.

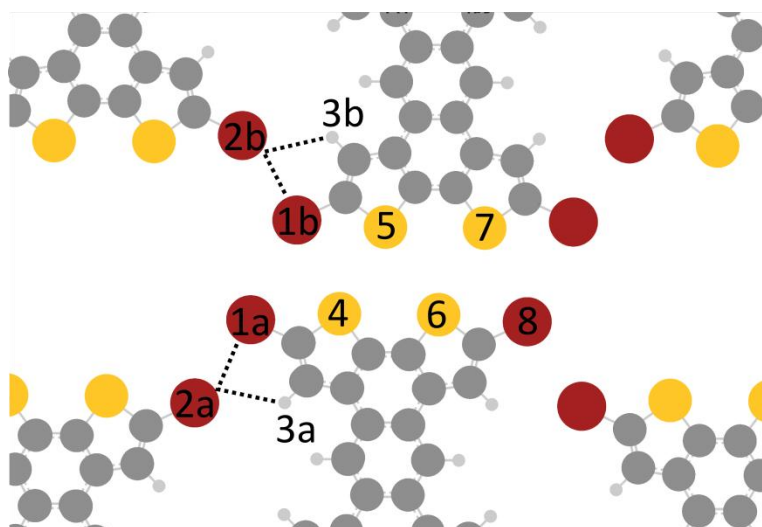
Compound 1:

Bond	Interacting orbitals	$\Delta E^{(2)}$ / kcal mol ⁻¹
D1 Br(1)⋯Br(2)	$n_{\text{Br}(1)} \rightarrow \sigma^*_{\text{C-Br}(2)}$	2.80
D2 Br(2)⋯H(3)	$n_{\text{Br}(2)} \rightarrow \sigma^*_{\text{C-H}(3)}$	2.17
D5 Br(1)⋯H(4)	$n_{\text{Br}(1)} \rightarrow \sigma^*_{\text{C-H}(4)}$	2.22
D4 Br(6)⋯S(7)	$n_{\text{Br}(6)} \rightarrow \sigma^*_{\text{C-S}(7)}$	0.53
D4 S(7)⋯Br(6)	$n_{\text{S}(7)} \rightarrow \sigma^*_{\text{C-Br}(6)}$	1.24
D3 Br(6)⋯S(8)	$n_{\text{Br}(6)} \rightarrow \sigma^*_{\text{C-S}(8)}$	0.83
D6 S(8)⋯S(9)	$n_{\text{S}(8)} \rightarrow \sigma^*_{\text{C-S}(9)}$	0.85
D6 S(9)⋯S(8)	$n_{\text{S}(9)} \rightarrow \sigma^*_{\text{C-S}(8)}$	0.85



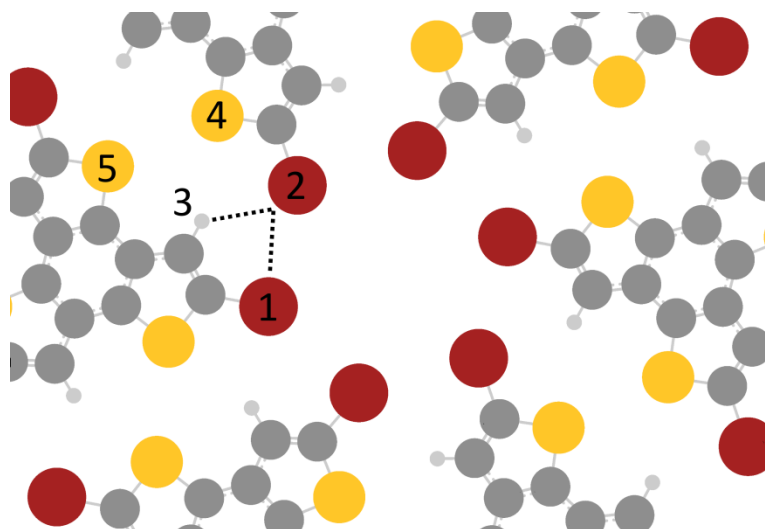
Compound 2:

Bond	Interacting orbitals	$\Delta E^{(2)} / \text{kcal mol}^{-1}$
D1a Br(1a)⋯Br(2a)	$n_{\text{Br}(1a)} \rightarrow \sigma^*_{\text{C-Br}(2a)}$	1.81
D2a Br(2a)⋯H(3a)	$n_{\text{Br}(2a)} \rightarrow \sigma^*_{\text{C-H}(3a)}$	0.46
D1b Br(1b)⋯Br(2b)	$n_{\text{Br}(1b)} \rightarrow \sigma^*_{\text{C-Br}(2b)}$	1.70
D2b Br(2b)⋯H(3b)	$n_{\text{Br}(2b)} \rightarrow \sigma^*_{\text{C-H}(3b)}$	0.66
Br(1a)⋯Br(1b)	$n_{\text{Br}(1a)} \rightarrow \sigma^*_{\text{C-Br}(1b)}$	0.51
Br(1b)⋯S(4)	$n_{\text{Br}(1b)} \rightarrow \sigma^*_{\text{C-S}(4)}$	1.59
D3 S(4)⋯S(5)	$n_{\text{S}(4)} \rightarrow \sigma^*_{\text{C-S}(5)}$	1.27
D3 S(5)⋯S(4)	$n_{\text{S}(5)} \rightarrow \sigma^*_{\text{C-S}(4)}$	0.80
D4 S(5)⋯S(6)	$n_{\text{S}(5)} \rightarrow \sigma^*_{\text{C-S}(6)}$	0.61
D4 S(6)⋯S(5)	$n_{\text{S}(6)} \rightarrow \sigma^*_{\text{C-S}(5)}$	0.61
D5 S(6)⋯S(7)	$n_{\text{S}(6)} \rightarrow \sigma^*_{\text{C-S}(7)}$	0.80
D5 S(7)⋯S(6)	$n_{\text{S}(7)} \rightarrow \sigma^*_{\text{C-S}(6)}$	1.27
D6 Br(8)⋯S(7)	$n_{\text{Br}(8)} \rightarrow \sigma^*_{\text{C-S}(7)}$	1.59



Compound 3:

Bond	Interacting orbitals	$\Delta E^{(2)} / \text{kcal mol}^{-1}$
D1 Br(1)⋯Br(2)	$n_{\text{Br}(1)} \rightarrow \sigma^*_{\text{C-Br}(2)}$	1.22
D2 Br(2)⋯H(3)	$n_{\text{Br}(2)} \rightarrow \sigma^*_{\text{C-H}(3)}$	1.83
D4 S(4)⋯H(3)	$n_{\text{S}(4)} \rightarrow \sigma^*_{\text{C-H}(3)}$	0.48
D3 S(4)⋯S(5)	$n_{\text{S}(4)} \rightarrow \sigma^*_{\text{C-S}(5)}$	0.70
D3 S(5)⋯S(4)	$n_{\text{S}(5)} \rightarrow \sigma^*_{\text{C-S}(4)}$	0.70



Additional STM Images

Figure S1. Large-scale STM topographs of **1**, **2**, and **3**. Domains of **1** and **2** are larger and more stable than domains of **3**. Fluctuations in domain boundaries are commonly observed for **3**.

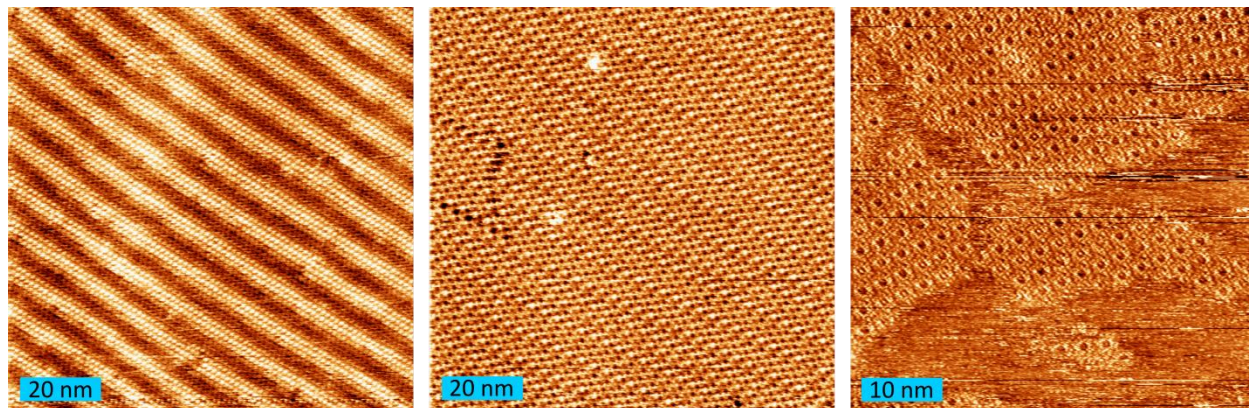


Figure S2. STM topographs in which both the graphite substrate and the molecular suprastructure are imaged, corrected for thermal drift. (a) **1**, (b) **2**, and (c) **3**. FFT images show peaks both due to the substrate (red circles) and the suprastructure (green circles).

